

Supplemental Information

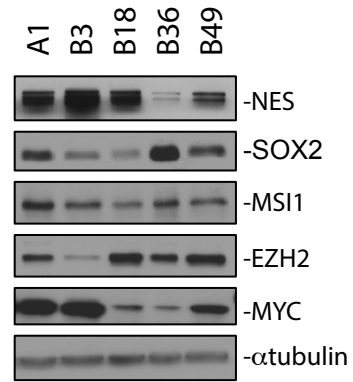
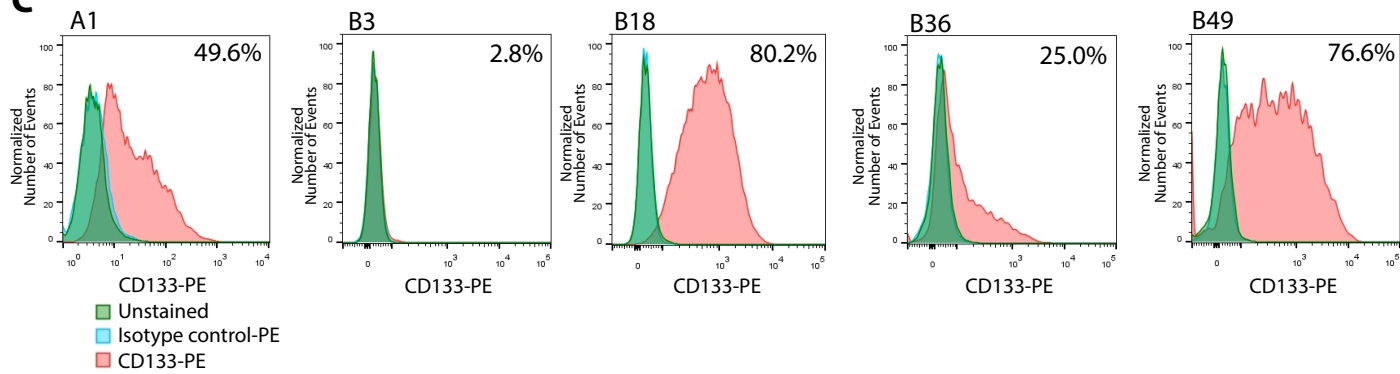
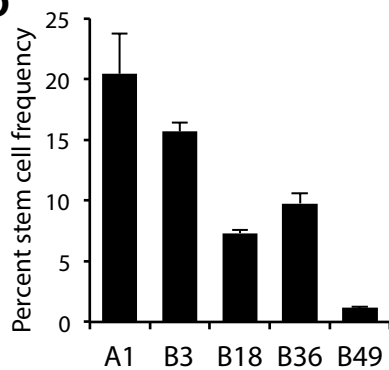
Supplemental Data

GSC line	Pathology of tumor	Clinical status
A1	GBM	Primary, right temporal lobe
B3	GBM	Primary, right temporo-parietal lobes
B18	GBM	Recurrent, right frontal lobe, (distant from primary left frontal lobe site)
B36	GBM with oligodendroglioma component	Primary, left temporal lobe
B49	GBM	Primary, right temporal

Table S1. Clinical characteristics of glioblastoma tumors used to derive GSCs, Related to Figure 1.

A

LINE	% NES+	% SOX2+
A1	94.7±4.0	77.2±3.4
B3	97.7±2.0	86.8±4.6
B18	97.8±3.8	90.6±8.1
B36	99.1±1.2	78.4±4.1
B49	99.3±0.6	93.1±6.0

B**C****D****E***In vivo tumorigenicity*

LINE	Cell number injected	No. of mice bearing tumor
A1	500,000	2/2
B3	250,000	3/3
B18	250,000	4/4
B36	250,000	3/3
B49	250,000	3/3

F

GENE	A1	B3	B18	B36	B49
DLL3	228.574	909.66	61.1034	144.332	195.467
OLIG2	1146.55	1397.82	79.2318	58.6081	165.988
ASCL1	491.917	2503.82	154.289	24.6639	276.56
NCAM1	524.634	443.575	546.287	332.409	143.015
CHI3L1	59.4892	6128.8	382.796	40.9617	465.355
SERPINE1	1268.51	470.792	2396.3	4889.08	1542.15
TIMP1	13486.8	14828.3	19748.5	9444	9327.74
TGFBI	2564.55	242.111	7185.31	1990.67	7805.91

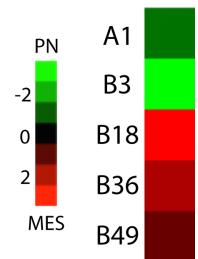


Figure S1. Characteristics of human glioblastoma stem-like lines used in this study, Related to Figure 1.

(A) Human GSC lines were subjected to Nestin and SOX2 immunofluorescence. Percent immunopositive cells was calculated by dividing by total number nuclei by Hoechst 33342. Data represent mean \pm SEM (n = 3).

(B) Cell lysates from human GSC lines were subjected to immunoblot analysis using indicated antibodies.

(C) Human GSC lines were dissociated and subjected to CD133-PE labeling followed by flow cytometry. A representative plot is shown from two independent experiments for each line. The mean CD133+ percentage from two experiments is shown in the top right corner of each plot.

(D) Human GSC lines were subjected to the extreme limiting dilution assay to determine the frequency self-renewing cells. Data represent mean+SEM (n = 3).

(E) GSC lines were injected into the right putamen of NOD-SCID (B18) or NOD-SCID γ (A1, B3, B36, B49) mice, and mice were sacrificed at 2-3 months. Brains were processed for Nestin and GFAP immunofluorescence to assess for tumor formation (Figure 1B and data not shown). All lines tested were capable of generating orthotopic xenograft tumors.

(F) Left: Mean normalized Illumina HT12v4 gene expression data for four Proneural and Mesenchymal signature GSC genes as described by Bhat et al. (2013) are shown for each GSC line from two independent experiments. Right: Expression for each gene was Z-corrected, and then the Proneural gene composite score was subtracted from the Mesenchymal gene composite score for each line and plotted as a heatmap to determine molecular subtype (Bhat et al., 2013).

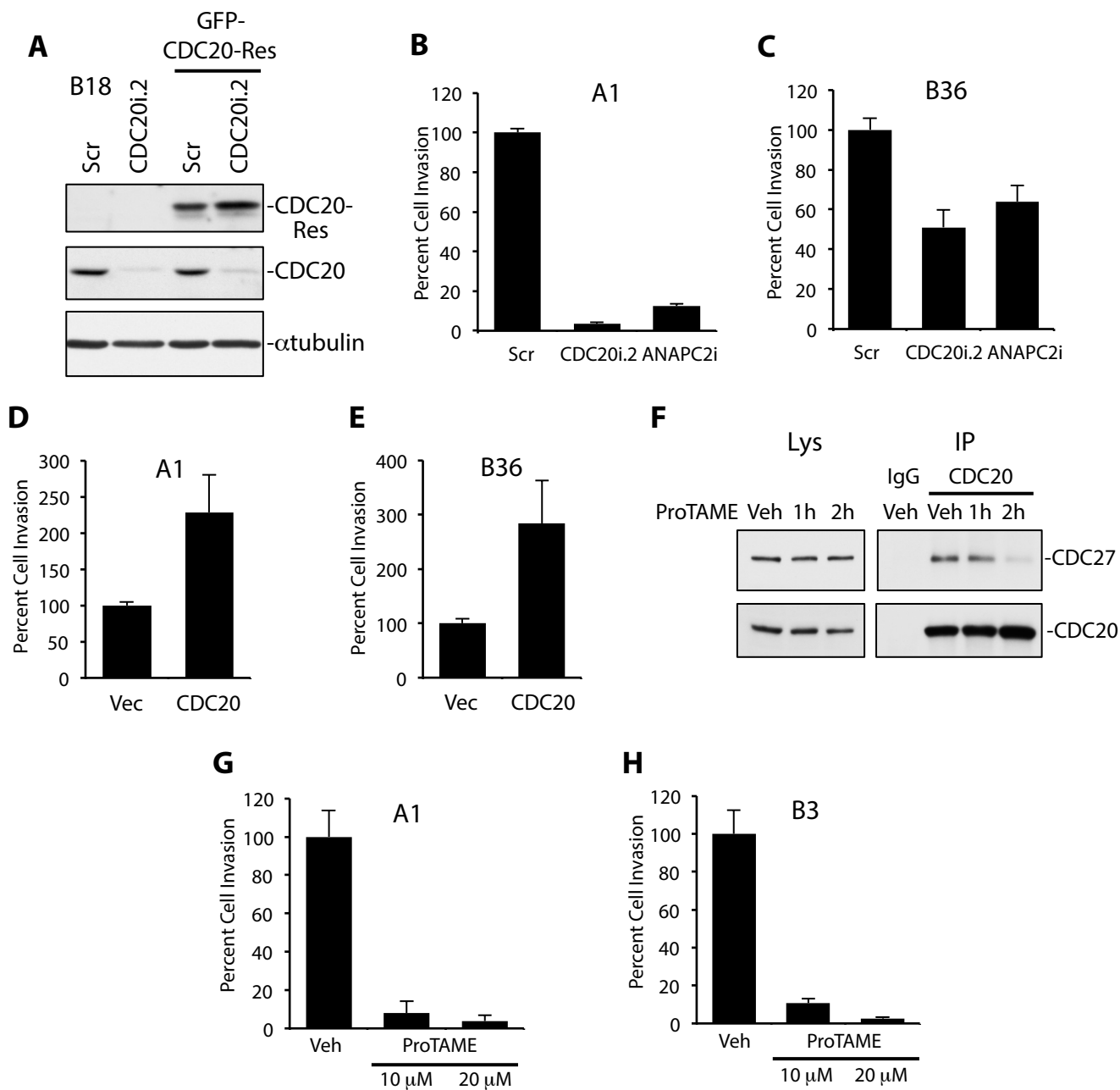


Figure S2. CDC20-APC is required for human GSC invasiveness *in vitro*, Related to Figure 1.

(A) GSCs were transduced with the indicated lentiviruses, and seven days later, cell lysates were subjected to immunoblot analysis using indicated antibodies. Whereas endogenous CDC20 is efficiently knocked down by CDC20i.2, GFP-CDC20-Res is resistant to CDC20 RNAi.

(B) A1 GSCs treated with the indicated RNAi lentiviruses (Scr = control scrambled SH002 virus) were subjected to the *in vitro* Matrigel transwell assay six days after infection to monitor invasiveness. Data represent mean+SEM (n = 3). CDC20 RNAi and ANAPC2 RNAi inhibited GSC invasiveness compared to control infection (ANOVA, $P < 0.0001$).

(C) B36 GSCs treated with the indicated RNAi lentiviruses were subjected to the *in vitro* Matrigel transwell assay six days after infection. Data represent mean+SEM (n = 4). CDC20 RNAi and ANAPC2 RNAi inhibited GSC invasiveness compared to control infection (ANOVA, $P \leq 0.001$).

(D) A1 GSCs treated with GFP-tagged CDC20-expressing lentivirus or control vector virus (Vec) were subjected to the *in vitro* Matrigel transwell assay as in (B). Data represent mean+SEM (n = 4). CDC20 overexpression increased the invasive capacity of GSCs compared to control infection (unpaired t-test, $P < 0.02$).

(E) B36 GSCs treated with GFP-tagged CDC20-expressing lentivirus or control vector virus were subjected to the *in vitro* Matrigel transwell assay as in (B). Data represent mean+SEM (n = 3). CDC20 overexpression increased the invasive capacity of GSCs compared to control infection (unpaired t-test, $P < 0.05$).

(F) B18 GSCs were treated with APC inhibitor ProTAME (20 μ M) or DMSO (Veh) for indicated times, and cell lysates were subjected to co-immunoprecipitation with anti-CDC20 or control IgG. Immunoprecipitates were resolved by SDS-PAGE and subjected to immunoblot analysis using indicated antibodies.

(G) A1 GSCs were subjected to the *in vitro* Matrigel transwell assay over 24 hours in the presence of indicated concentrations of ProTAME or DMSO (Veh). Data represent mean+SEM

(n = 3). APC inhibitor ProTAME inhibited A1 GSC invasiveness in a dose-dependent manner (ANOVA, $P < 0.0001$).

(H) B3 GSCs were subjected to the *in vitro* Matrigel transwell assay over 24 hours in the presence of indicated concentrations of ProTAME or DMSO (Veh). Data represent mean+SEM

(n = 3). APC inhibitor ProTAME inhibited B3 GSC invasiveness in a dose-dependent manner (ANOVA, $P < 0.0001$).

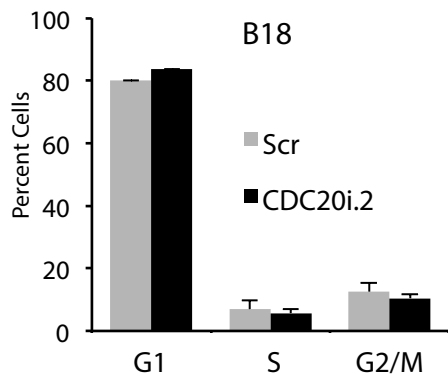
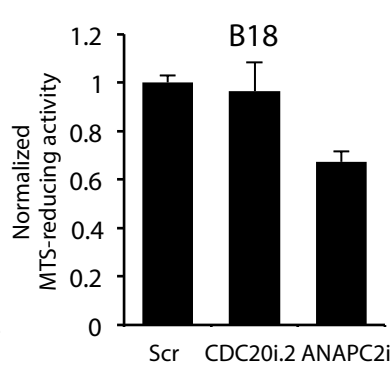
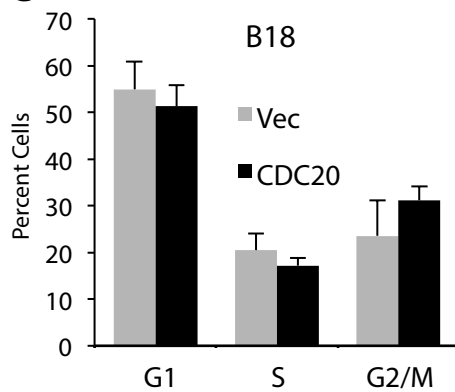
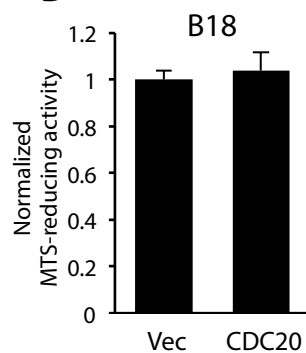
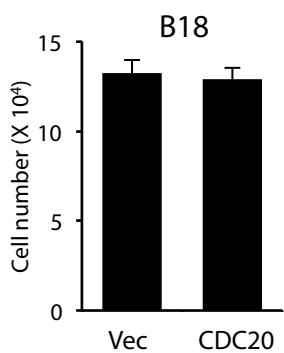
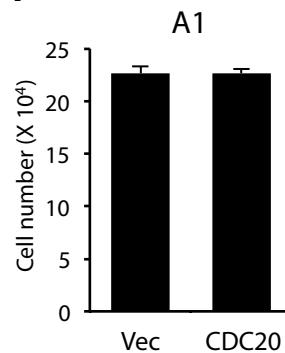
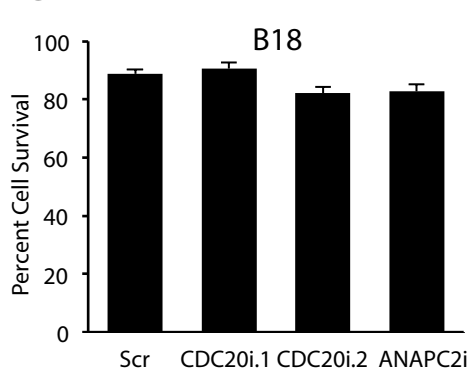
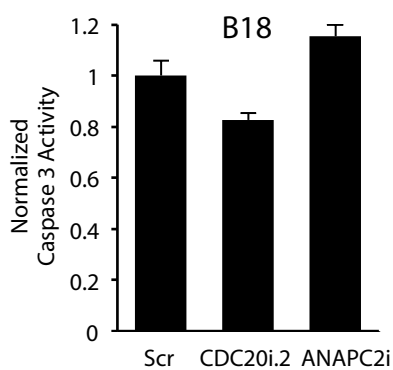
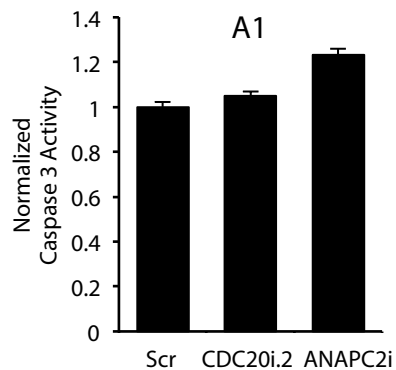
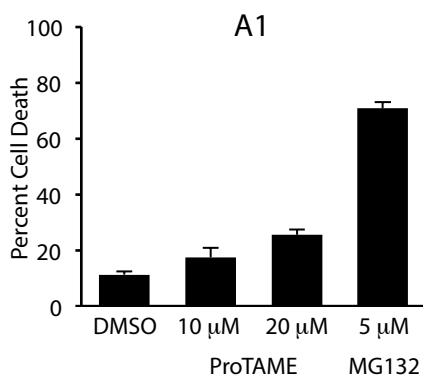
A**B****C****D****E****F****G****H****I****J**

Figure S3. The effect of molecular and pharmacological manipulations of CDC20-APC on cell cycle distribution, proliferation, cell death, and cell health, Related to Figure 1.

(A) GSCs transduced with *CDC20* RNAi (CDC20i.2) or control scrambled (Scr) lentivirus were subjected to propidium iodide DNA labeling seven days later followed by flow cytometry to assess the distribution of cell cycle phases. Scr = control scrambled lentivirus. Data represent mean+SEM (n = 2). *CDC20* knockdown did not significantly alter the cell cycle profile of GSCs compared to control infection. (ANOVA, $P \geq 0.222$).

(B) GSCs infected with the indicated RNAi lentiviruses or control scrambled virus were subjected to the MTS cellular viability/proliferation assay seven days later. Data represent mean+SEM (n = 3). *CDC20* RNAi did not significantly alter cellular proliferation compared to control infection (ANOVA, $P = 0.717$). *ANAPC2* RNAi significantly decreased cellular proliferation compared to control infection (ANOVA, $P = 0.004$).

(C) GSCs transduced with GFP-tagged *CDC20*-expressing (CDC20) or control vector (Vec) lentivirus for five days were assayed as in (A). Data represent mean+SEM (n = 2). *CDC20* overexpression did not significantly alter the cell cycle profile of GSCs compared to that of control infection. (ANOVA, $P \geq 0.284$).

(D) GSCs transduced with GFP-tagged *CDC20*-expressing (CDC20) or control vector (Vec) lentivirus for five days were assayed as in (B). Data represent mean+SEM (n = 3). *CDC20* overexpression did not significantly alter cellular viability/proliferation as monitored by the MTS assay compared to control infection. (ANOVA, $P = 0.69$).

(E) B18 GSCs treated as in (C) were plated in 24-well plates, and seven days later, the number of live cells was counted by Trypan blue exclusion. Data represent mean+SEM (n = 3). *CDC20* overexpression did not significantly alter cell number compared to control infection (unpaired t-test, $P = 0.74$).

(F) A1 GSCs treated as in (C) were processed as in (E). Data represent mean+SEM (n = 3). CDC20 overexpression did not significantly alter cell proliferation compared to control infection (unpaired t-test, $P = 1.0$).

(G) GSCs were transduced with indicated RNAi lentiviruses or control scrambled (Scr) lentivirus, and live cell counts were quantified by Trypan blue exclusion six days later. Data represent mean+SEM (n = 3). CDC20 knockdown (CDC20i.1 and CDC20i.2) did not significantly alter cell survival in GSCs compared to control infection. (ANOVA, $P \geq 0.09$). ANAPC2 knockdown did not significantly alter cell survival in GSCs compared to control infection. (ANOVA, $P = 0.064$).

(H) B18 GSCs were transduced with indicated RNAi lentiviruses or control scrambled (Scr) lentivirus, and caspase-3 activity was quantified by a fluorometric assay. The caspase-3 signal was divided by the total nuclear count (Hoechst 33342) and normalized to control infection (=1). Data represent mean+SEM (n = 3). CDC20 knockdown did not significantly alter caspase-3 activity in GSCs compared to control infection with a trend towards decreased caspase-3 activity. (ANOVA, $P = 0.04$). ANAPC2 knockdown did not significantly alter caspase-3 activity in GSCs compared to control infection. (ANOVA, $P = 0.06$).

(I) A1 GSCs were transduced with indicated RNAi lentiviruses or control scrambled (Scr) lentivirus, and caspase-3 activity was quantified by a fluorometric assay as in (H). Data represent mean+SEM (n = 3). CDC20 knockdown did not significantly alter caspase-3 activity in GSCs compared to control infection (ANOVA, $P = 0.166$). ANAPC2 knockdown significantly increased caspase-3 activity in GSCs compared to control infection. (ANOVA, $P = 0.0001$).

(J) A1 GSCs were treated with the indicated concentrations of ProTAME for 48 hours and assessed for cell death by the LDH release assay. MG132 served as a positive control for cell death. Data represent mean+SEM (n = 3). 10 μ M ProTAME, which was sufficient to inhibit invasion (Figure S2G), did not significantly increase cell death compared to DMSO (Veh) control

(ANOVA, $P = 0.068$). 20 μM ProTAME triggered modest levels of cell death at 48 hours compared to Veh (ANOVA, $P = 0.0003$).

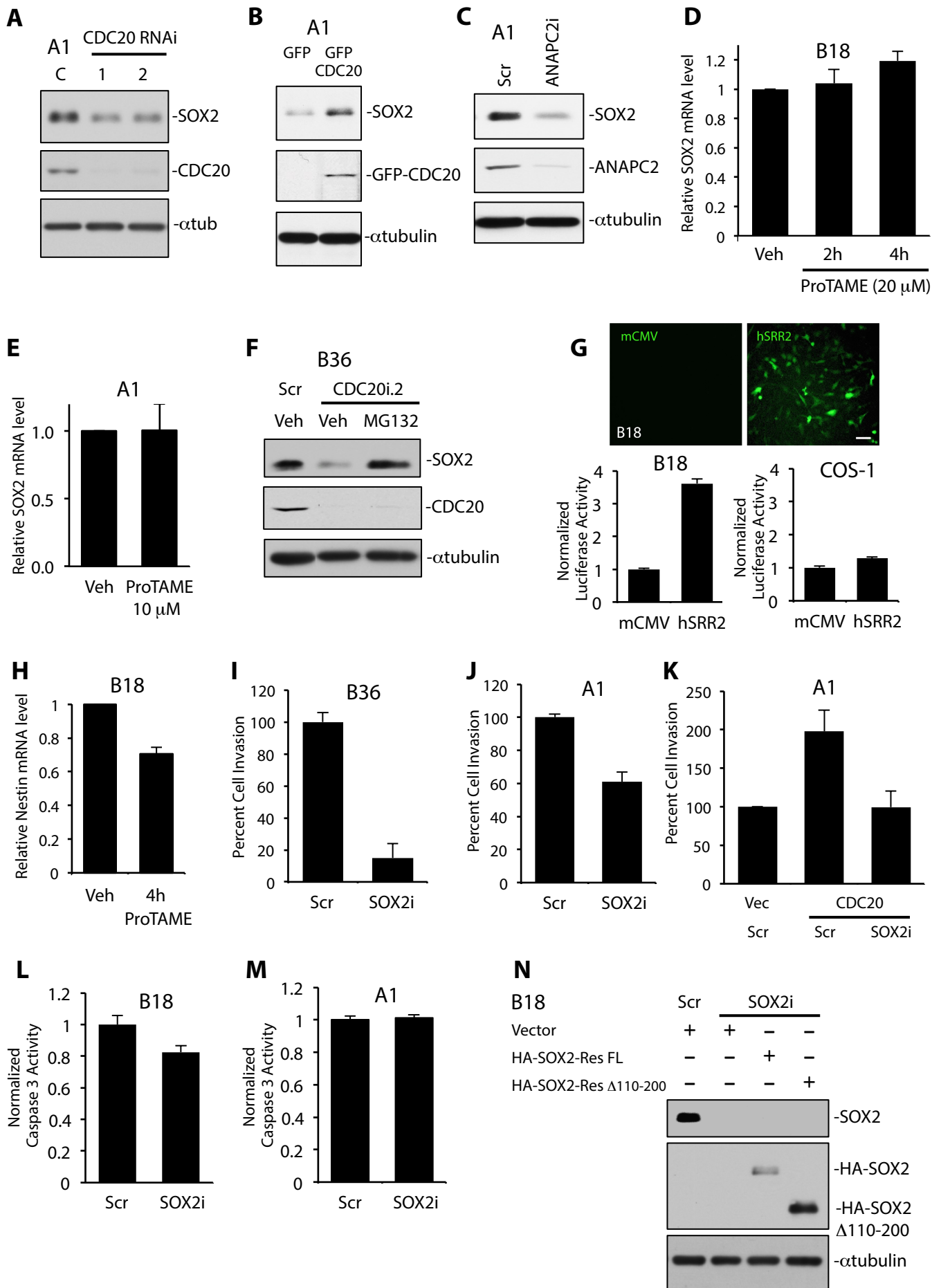


Figure S4. CDC20-APC controls SOX2 protein stability and SOX2-dependent transcription in GSCs, Related to Figure 3.

(A) A1 GSCs were transduced with *CDC20* RNAi (CDC20i.1 and CDC20i.2) or control LacZ RNAi (C) lentivirus, and seven days later, cell lysates were subjected to immunoblotting using indicated antibodies.

(B) A1 GSCs were transduced with GFP-tagged *CDC20*-expressing lentiviruses or control GFP-expressing virus (GFP), maintained in RHB-A media for five days, and cell lysates were subjected to immunoblotting using indicated antibodies. Similar results were obtained using control N103 vector virus (data not shown).

(C) A1 GSCs were transduced with *ANAPC2* RNAi or control scrambled RNAi (Scr) lentivirus, and seven days later, cell lysates were subjected to immunoblotting using indicated antibodies.

(D) B18 GSCs were treated with 20 μ M of ProTAME or DMSO (Veh) for indicated time points, and RNA was harvested from treated cells and reverse transcribed into cDNA. qPCR was performed on samples using specific primers for human *SOX2*. *GAPDH* and *ACTB* were used as reference genes. Data represent mean+SEM (n = 3). ProTAME treatment did not significantly alter *SOX2* RNA levels (ANOVA, $P \geq 0.128$).

(E) A1 GSCs were treated with 10 μ M of ProTAME or DMSO (Veh), and RNA was harvested from treated cells and reverse transcribed into cDNA. qPCR was performed as in (D). Data represent mean+SEM (n = 5). ProTAME treatment did not significantly alter *SOX2* RNA levels (unpaired t-test, $P = 0.97$).

(F) B36 GSCs were transduced with *CDC20* RNAi (CDC20i.2) or control SHC002 (Scr) lentiviruses for seven days and then treated with 10 μ M of MG132 or DMSO (Veh) for 6 hours. Cell lysates were subjected to immunoblotting using indicated antibodies.

(G) Top: B18 GSCs stably infected with either control reporter (mCMV) or the *SOX2* reporter (hSRR2) were monitored for reporter activity by visualizing GFP using live fluorescence

microscopy. Scale bar = 50 μ m. Bottom: B18 GSCs stably infected with either control mCMV or hSRR2 reporter were assessed for luciferase activity by luminometry, and luciferase values were normalized by total protein (left). COS-1 cells stably infected with either control mCMV or hSRR2 reporter were assessed for luciferase activity by luminometry, and luciferase values were normalized by total protein (right). Data represent mean+SEM (n = 3). GSCs exhibited significant SOX2 reporter luciferase activity above control mCMV reporter (unpaired t-test, $P = 0.0006$).

(H) B18 GSCs were treated with 20 μ M of ProTAME or DMSO (Veh) for 4 hours, and RNA was processed as in (D). qPCR was performed by using primers specific for human Nestin. *GAPDH* and *ACTB* were used as reference genes. Data represent mean+SEM (n = 3). ProTAME decreased Nestin mRNA in GSCs compared to vehicle. (unpaired t-test, $P = 0.002$).

(I) B36 GSCs were transduced with SOX2 RNAi or control scrambled (Scr) lentiviruses and subjected to *in vitro* Matrigel invasion assays seven days later. Data represent mean+SEM (n = 5). SOX2 RNAi decreased GSC invasiveness compared to control infection (unpaired t-test, $P < 0.0001$).

(J) A1 GSCs were transduced with SOX2 RNAi or control scrambled (Scr) lentiviruses and subjected to *in vitro* Matrigel invasion assays seven days later. Data represent mean+SEM (n = 3). SOX2 RNAi decreased GSC invasiveness compared to control infection (unpaired t-test, $P < 0.0009$).

(K) A1 GSCs were transduced with SOX2 RNAi or control scrambled (Scr) lentiviruses along with CDC20-expressing or control vector (Vec) lentiviruses and subjected to *in vitro* Matrigel invasion assays seven days later. Data represent mean+SEM (n = 3). CDC20 overexpression + Scr increased GSC invasiveness compared to that of control infected cells, and SOX2 RNAi in the setting of CDC20 overexpression decreased invasiveness compared to that of CDC20 overexpression + Scr (ANOVA, both $P = 0.013$).

(L) B18 GSCs were transduced with SOX2 RNAi or control scrambled (Scr) lentivirus, and caspase-3 activity was quantified by a fluorometric assay as in Figure S3H. Data represent mean+SEM (n = 3). SOX2 knockdown did not significantly alter caspase-3 activity in GSCs compared to that of control infection (unpaired t-test, $P = 0.07$).

(M) A1 GSCs were transduced with SOX2 RNAi or control scrambled (Scr) lentivirus and caspase-3 activity was quantified by a fluorometric assay as in Figure S3H. Data represent mean+SEM (n = 3). SOX2 knockdown did not significantly alter caspase-3 activity in GSCs compared to that of control infection (unpaired t-test, $P = 0.73$).

(N) B18 GSCs transduced with SOX2 RNAi or control scrambled (Scr) lentiviruses were co-transduced with HA-tagged full-length SOX2-Res, SOX2-Res Δ 110-200, or control vector viruses, cell lysates were subjected to immunoblot analysis using the indicated antibodies seven days later.

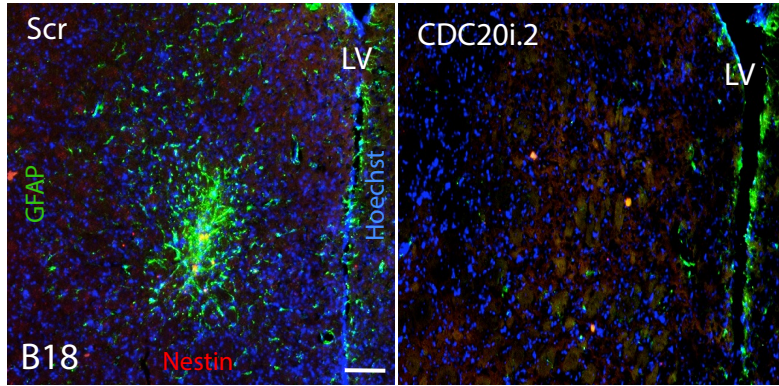
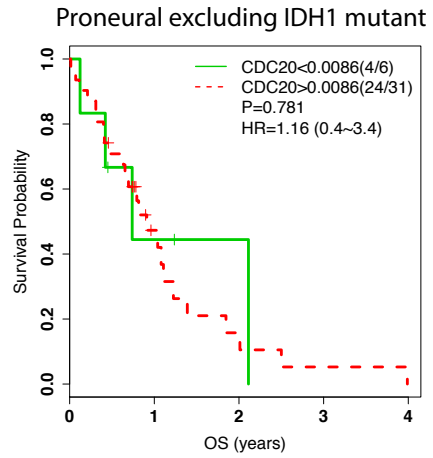
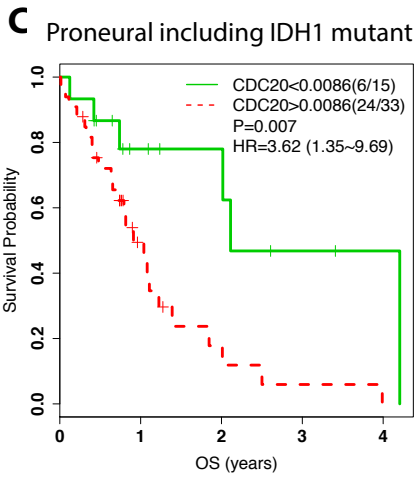
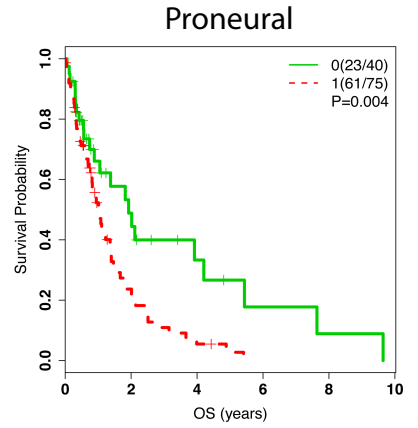
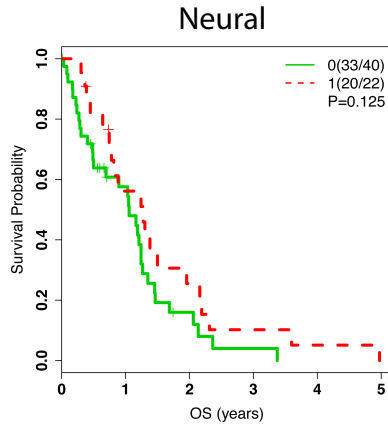
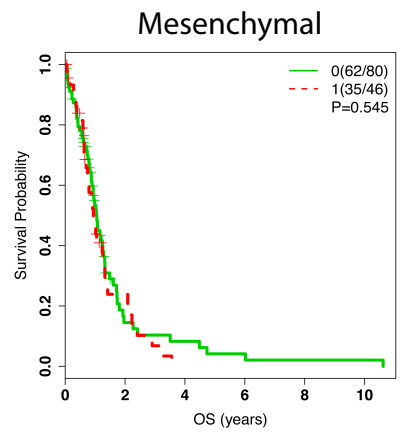
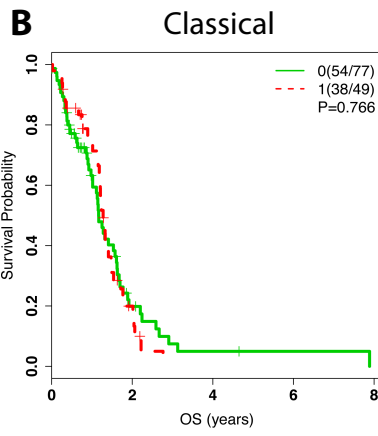
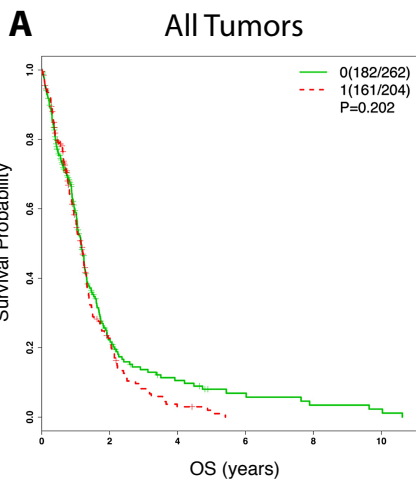


Figure S5. Visualization of GSC tumorigenicity *in vivo* by immunofluorescence, Related to Figure 4.

B18 GSCs were infected with *CDC20* RNAi (CDC20i.2) or control SHC002 (Scr) virus and selected with puromycin for 72 hours. 250,000 cells were injected per animal into the right putamen of NOD-SCID mice using a stereotactic apparatus. Three months after injection, animals were sacrificed. Brains were harvested, processed to generate 10 micron-thick frozen sections, and then subjected to immunohistochemistry using antibodies against Nestin and GFAP. Nuclei were stained with Hoechst 33342. Images of processed sections were obtained using fluorescence microscopy. LV = lateral ventricle. Scale bar = 100 μ m.



D Proneural glioblastomas

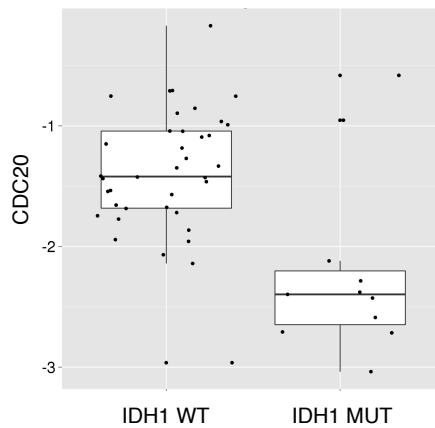


Figure S6. The impact of CDC20 expression on overall survival in the TCGA Glioblastoma dataset, Related to Figure 5.

(A) Kaplan-Meier curves showing overall survival (OS) of 466 newly diagnosed glioblastoma patients from the TCGA divided by normalized *CDC20* expression from the Agilent microarray (compared to normal samples). Stratification of patients using an optimized *CDC20* expression cut-point did not predict longer or short OS in the entire patient set (log-rank test, $P = 0.202$).

(B) Kaplan-Meier curves showing OS of patients separated by Classical, Mesenchymal, Neural, and Proneural glioblastoma subtype tumors from the TCGA based on normalized *CDC20* expression and stratification of patients into two groups using the same *CDC20* expression cut-point derived in (A). Consistent with the results using a 2-fold *CDC20* expression cut-off (Figure 5), the patient group with higher *CDC20* expression was associated with decreased OS specifically in patients with Proneural subtype tumors (log-rank test, $P = 0.004$).

(C) Kaplan-Meier curves showing overall survival (OS) of all 49 Proneural glioblastoma patients with available Agilent microarray and mutation data (both IDH1 MUT and WT) (left) and the 38 IDH1 WT patients only (right) stratified by an optimal *CDC20* expression cutoff identified by the derived linear predictor from a Cox model applied to Proneural patients only. When IDH1 MUT patients were included, patients with high *CDC20* exhibited a worse prognosis (HR=3.62, 95% CI:1.35~9.69, log rank test $P = 0.007$), but the survival curves of patients with *CDC20* high and low tumors were not significantly different when excluding IDH1 MUT patients (log rank test, $P = 0.781$).

(D) Box plot (median and middle 50% of data represented in each box) of *CDC20* expression in the 49 Proneural glioblastomas in the TCGA with available Agilent microarray and mutation data. IDH1 MUT tumors demonstrated significantly lower expression of *CDC20* compared to that of IDH1 WT tumors in the Proneural subgroup (mean IDH1 WT/IDH1 MUT *CDC20* mean = -1.38/-2.20, two sample t-test, $P = 0.005$, Wilcoxon rank sum test, $P = 0.001$)

Supplemental Experimental Procedures

Antibodies and drugs. Antibodies used for this study include polyclonal rabbit anti-CDC20 (H-175) (Santa Cruz Biotechnology) and mouse anti-CDC27 (C-4) (Santa Cruz Biotechnology), polyclonal rabbit anti-ANAPC2 (APC2 (H-295)) (Santa Cruz Biotechnology), mouse anti- β -Actin(C4) (Santa Cruz Biotechnology), polyclonal rabbit anti-Nestin (Millipore), mouse anti-Nestin MAB1259 (R&D systems), rabbit anti-Nestin ABD69 (Millipore), monoclonal rabbit anti-SOX2 86D9 (Cell Signaling Technology), rabbit polyclonal anti GFAP Z0334 (Dako), mouse anti- α -tubulin(Sigma), and polyclonal rabbit anti-GFP serum (A6455) (Molecular Probes, Life Technologies), monoclonal rabbit anti-EZH2 D2C9 (Cell Signaling Technology), mouse anti-BMI1 05-637 (Millipore), polyclonal rabbit anti-myc (A-14) (Santa Cruz Biotechnology), mouse anti-myc (9E10) (SIGMA), monoclonal rabbit anti-c-MYC D84C12 (Cell Signaling Technology), rabbit anti-MSI1 ab21628 (Abcam), and mouse anti-FLAG (M2) (SIGMA). CD133/1(AC133) antibody conjugated to PE was purchased from Miltenyi Biotec Inc. Drug used include cell-permeable APC inhibitor ProTAME (Boston Biochem) proteasome inhibitor MG-132 (EMD Millipore Corporation), and bortezomib. Hoechst 33342 was purchased from Molecular Probes, Life Technologies, and propidium iodide and Fluoroshield with DAPI purchased from SIGMA.

Plasmids. The following human gene target-directed shRNA plasmids (in pLKO.1) from the RNAi Consortium were used: *CDC20* RNAi (CDC20i.1 and 2), targeting 5'-AGACCAACCCATCACCTCAGT-3' and 5'-TGGTGGTAATGATAACTTGGT-3', respectively (Washington University RNAi Core); *ANAPC2* RNAi, targeting 5'-CCCGGCACCTTCTCTGTCATT-3'; *SOX2* RNAi, targeting 5'-AGCGTGACTTATCCTTCTTC-3' (SIGMA); LacZ RNAi, targeting 5'-TGTTTCGCATTATCCGAACCAT-3'; control RNAi plasmids SHC002 and Scrambled containing sequences CCGGCAACAAGATGAAGAGCACCAACTCGAGTTGGTGCTCTTCATCTTGTTGTTTTT

and CCTAAGGTAAAGTCGCCCTCGCTCGAGCGAGGGCGACTTAACCTTAGG (Addgene), respectively. Plasmids encoding FLAG-tagged rat Cdc20, the N-terminal GFP and rat Cdc20 fusion protein (GFP-CDC20-Res) as well as GFP-NLS-CDC20-Res and GFP-NES-CDC20-Res have been described (Kim et al., 2009). GFP-CDC20-Res and mutant GFP-CDC20-Res cDNAs were subcloned into N103 lentiviral vector (kindly provided by Dr. Andrew Yoo (Washington University)). Full-length human SOX2 was cloned from a B18 GSC cDNA library. Myc epitope-tagged rat Cdc20 deletion and human SOX2 deletion expression plasmids were generated in pcDNA3 by standard PCR and subcloning techniques. GST-human SOX2 and GST-CDC20(WD40) were generated by using the bacterial expression plasmid pGEX-4T1. The HA-tagged full-length human SOX2 rescue construct (HA-SOX2-Res), which harbors 7 base mismatches in the region targeted by SOX2 RNAi (GAAAAAAGACAAATATACCTT, mismatches highlighted), and SOX2 deletion mutants were generated by gene synthesis (Integrated DNA Technologies) and subcloned into pcDNA3 and N103. The human SOX2 regulatory region 2 (hSRR2)/minimal CMV promoter (mCMV)-driven GFP T2A luciferase lentiviral plasmid was generated by first PCR cloning SRR2 from 293 cell genomic DNA using the following primers: forward: CCATCGATTTTTAGGATAACATTGTACTGGGAAG and reverse: CCACTAGTTATCAAAAGCATTTATATTTGCAAAC. The PCR product was then subcloned into the Clal and SpeI sites in pGreenfire1 mCMV-GFP T2A luciferase plasmid (Systems Biosciences). CMV-driven GFP T2A luciferase lentiviral plasmid was generated by standard PCR subcloning. All plasmids were confirmed by sequencing.

Real-Time Quantitative PCR. RNA was isolated using the RNeasy Plus Mini Kit (QIAGEN). Reverse transcription was performed with High-Capacity cDNA Reverse Transcription Kit (Applied Biosystems). Power SYBR Green PCR Master Mix (Applied Biosystems) was used for amplification on the CFX Connect Real-Time System (Bio-Rad). All samples were run in triplicate with a corresponding β -Actin and glyceraldehyde-3-phosphate dehydrogenase

(GAPDH) control for each. Relative transcript copy number for each transcript was normalized to β -Actin and GAPDH and was calculated using the $\Delta\Delta Cq$ method. The primers sets used for each gene are as follows: Human *SOX2* forward: 5'-GGGGAAAGTAGTTTGCTGCC-3'; Human *SOX2* reverse: 5'-CGCCGCCGATGATTGTTATT-3'; Human *NES* forward: 5'-GAGAGCCCTGAGCCCAAAGA-3'; Human *NES* reverse: 5'-CTCCCGCAGCAGACTCACC; Human β -Actin forward: 5'-ATGATATCGCCGCGCTCGTCGTC-3'; Human β -Actin reverse: 5'-TGACCCATGCCACCATCACG-3'; Human *GAPDH* forward: 5'-ATGGGGAAGGTGAAGGTCG-3'; Human *GAPDH* reverse: 5'-GGGGTCATTGATGGCAACAATA-3'.

Transient transfection. Polyethyleneimine (PEI, Polysciences #24765-2) was dissolved in ddH₂O to a concentration of 1 mg/mL. The solution was then adjusted to pH 7.0 and filter sterilized. A mixture of plasmid DNA and PEI solution (1:4:: μ g DNA: μ L PEI) was made in OPTIMEM (Life Technologies) and incubated at room temperature for 15 minutes. Total plasmid DNA amount was equalized by addition of vector pcDNA3. DNA/PEI complexes were applied to cells, and media was changed after 12-16 hours. Experiments were performed 24-36 hours following transfection.

Lentiviral production. 293LE cells were plated with a goal density of 70-80% after 1 day. The next day, transfection was performed using the PEI transfection method to introduce the plasmid of interest along with packaging plasmid psPAX2 and envelope plasmid pCMV-VSVG to Opti-MEM (Life Technologies). On day 6, medium from the plates was collected and spun down at 1200 x g for 5 min at 4°C. Supernatant was filtered through 0.45 micron filters. Lenti-X Concentrator (Clontech) was then added to the filtrate and mixed, and the tubes were incubated at 4°C for 6-7 hours. Lentiviruses were then centrifuged at 1500 x g for 45 minutes at 4°C.

Supernatant was aspirated; pellets were re-suspended in one tenth of the original medium volume of cold PBS, and stored at -80°C in aliquots. Viral copy number was adjusted for transduction of GSCs on the basis of titer measured using the Lenti-X qRT-PCR titration kit (Clontech).

Co-immunoprecipitation and immunoblot analysis. Cells were lysed in 1% NP-40 lysis buffer containing 20 mM Tris [pH 8], 200 mM NaCl, 10% glycerol, 1 mM EDTA, 10 mM NaF, 1 mM sodium orthovanadate, and a protease inhibitor cocktail (Calbiochem). Clarified lysates were precleared with protein A/G-sepharose (Life Technologies), and immunoprecipitations were performed overnight at 4° with indicated antibodies followed by protein A/G-sepharose. Pellets were washed 6 times with lysis buffer and boiled in Laemmli sample buffer. Samples were separated by SDS-PAGE and transferred to 0.45 µm Immobilon-P PVDF membrane (EMD Millipore). Membranes were blocked in 5% Milk in Tris-buffered saline with Tween-20 (TBST) at room temperature and incubated with primary antibodies at 4°C overnight or at room temperature for 2-4 hours. Membranes were washed with TBST and incubated with appropriate horseradish peroxidase-conjugated secondary antibodies for 1 hour at room temperature. Membranes were then washed with TBST and developed using Pierce ECL western blotting substrate (Thermo Scientific).

***In vitro* binding.** GST-human SOX2 and the corresponding GST control proteins were bacterially expressed and isolated using Glutathione Sepharose 4 Fast Flow (GE Healthcare) according to manufacturer's instructions. GST-CDC20(WD40) and the corresponding GST proteins were produced in transiently transfected 293 cells following a similar protocol as for bacterially expressed proteins. Using the pcDNA3-myc-rat Cdc20 and pcDNA3-myc or HA-human SOX2 deletion mutant plasmids, ³⁵S-labeled products were *in vitro* translated with the TNT-coupled reticulocyte lysate system (Promega) and incubated with indicated GST-fusion

proteins bound to glutathione-sepharose 4 Fast Flow beads in 1% NP-40 lysis buffer at 4°C for 16 hours (GE Healthcare). The beads were washed 6 times with lysis buffer and boiled in Laemmli sample buffer. Proteins were resolved by SDS-PAGE, and ³⁵S-labeled proteins were visualized by autoradiography with signal enhancement (Amplify, GE Healthcare). GST-fusion proteins were assessed by Coomassie Brilliant Blue R-250 (Biorad).

Flow cytometry for CD133. 5×10^5 live GSCs were dissociated and labeled with CD133/1(AC133) antibodies conjugated to PE or mouse IgG1 isotype control antibodies conjugated to PE (Miltenyi Biotec Inc). Normal mouse serum (SIGMA) was used as blocking reagent. Cells were subjected to flow cytometry (Siteman Flow Cytometry Core) using the Blue fluorescence-2 channel to detect PE and analyzed using Flowjo 10.

Cell survival and proliferation. 2×10^4 GSCs were plated per well in a 24-well plate. Fresh medium was added every 2 or 3 days. One week after plating, cells were assessed for the number of viable cells as determined by Trypan blue exclusion (Life Technologies) was quantified using the Countess Automated Cell Counter (Life Technologies).

MTS assay. 3-(4,5-dimethylthiazol-2-yl)-5-(3-carboxymethoxyphenyl)-2-(4-sulfophenyl)-2H-tetrazolium (MTS) assays were performed per manufacturer's instructions (Promega), and MTS-reducing activity was normalized for each condition to control scrambled RNAi or vector lentiviruses as appropriate (=1).

Cell cycle analysis. GSCs were plated at a density of 2×10^5 /60mm dish 18 hrs prior to transduction with *CDC20* RNAi or *CDC20* overexpression virus. Cells were fixed with 50% Ethanol/ phosphate-buffered saline (PBS)/0.01% IGEPAL CA-630 overnight at 4°, treated with Trypsin, RNase, and then spermine. DNA nuclei were stained with propidium iodide. Cells were then assessed using FACScan (BD Bioscience) (Siteman Flow Cytometry Core) with

fluorescence-2 (FL2) detector to detect light emitted between 564 and 604 nm. The data were analyzed using Flow Jo 10 software.

Cell death assays. The lactate dehydrogenase (LDH) release assay has been described previously (Kim et al., 2002). Briefly, LDH values were normalized by subtracting the background LDH released by control cells from treated cells and scaling to the signal triggered by complete cell death induced by 24 hours exposure to 30 mM of A23187.

Caspase-3 activity assay. 4×10^4 cells were plated in 24-well plates in triplicate per experiment. One day after plating, cells were transduced with indicated lentiviruses. Puromycin was added to the culture medium 24 hours after transduction and the cells were incubated for an additional 6 days. On day 7 after viral transduction, 200 μ l of Caspase-Glo 3/7 Reagent (Promega G8091) was added to 200 μ l of culture media per well. Plates were mixed on a plate shaker for 30 seconds then allowed to incubate at room temperature for 1 hour, and luminescence readings were acquired (TECAN Infinite M200 Pro).

Immunocytochemistry. Polyornithine and laminin-coated German glass coverslips (Bello Glass, Inc) were seeded with 2×10^4 GSCs in a 24-well plate. Cells were fixed with 4% paraformaldehyde for 15 minutes at room temperature and subjected to immunofluorescence analysis with indicated antibodies according to standard protocols.

Immunohistochemistry. At the indicated time post-injection, animals were sacrificed, and brains harvested for analysis. Brains were fixed in 4% paraformaldehyde and placed in 30% sucrose for cryoprotection. 10 micron-thick frozen sections were generated using a cryostat. Frozen sections were fixed in ice-cold acetone and then rehydrated in PBS. Sections were blocked in PBS containing 4% normal goat serum (Vector laboratories) for 1 hour at room temperature. Double immunostaining for Nestin and GFAP or single immunostaining for GFP

was then carried out overnight at 4°C, and sections were washed with PBS and incubated with appropriate secondary antibodies conjugated to fluorescent dyes (Alexa Fluor 568 Goat Anti-Mouse, Alexa Fluor 488 Goat Anti-Rabbit (Life Technologies) for 60 minutes at room temperature. After additional PBS washes, Hoechst 33342 or DAPI was added to sections to stain nuclei. Mounting medium was then added to the sections, and slides were cover-slipped. Fluorescent images of the sections were taken using an automated inverted microscope (Leica Microsystems, Cat. No. DMI4000 B). For whole coronal brain images, processed sections were imaged using the Zeiss ApoTome microscope (Histology and Microscopy Core, Washington University). Multichannel images of section parts were initially acquired using the blue, FITC, and rhodamine (Cy3) channels in multidimensional acquisition. The acquired images were then merged to obtain the image of the whole brain section.

***In vitro* luciferase assay.** Cells seeded on PLO and laminin-coated 24-well Primaria plates stably infected with pGreenfire1 hSRR2/mCMV-GFP T2A luciferase or control pGreenfire1 mCMV-GFP T2A luciferase lentivirus was transduced with indicated RNAi viruses and selected with puromycin. Seven days later, cells were visualized for GFP expression by live fluorescence microscopy and then assayed for luciferase activity using the One-Glo system (Promega). Luciferase signal was quantified by luminometry using a Tecan Infinite M200 Pro Microplate Reader and divided by total protein levels. Data were normalized to the control condition (Scr + mCMV-GFP T2A luciferase infection = 1).

Live bioluminescence imaging. GSCs stably expressing GFP T2A luciferase by lentiviral transduction were then infected with indicated lentiviruses and injected into the brains of NOD-SCID γ mice as above. For bioluminescence imaging, animals were given 150 mg/mL D-luciferin (Gold Biotech) in PBS and imaged with a charge-coupled device (CCD) camera-based bioluminescence imaging system (IVIS Lumina; Caliper, Hopkinton, MA; exposure time 3-5

minutes, binning 8, field of view 12, f/stop 1, open filter) (Molecular Imaging Center, Washington University). Signal was displayed as photons/sec/cm²/sr (Gross and Piwnica-Worms, 2005).

TCGA analysis. Glioblastoma clinical and Agilent G4502A gene expression microarray data was obtained for 483 glioblastoma tumors (including 10 normal brain tissue samples) from The Cancer Genome Atlas (TCGA) (<http://cancergenome.nih.gov/>). The subtype classification as defined by Verhaak and colleagues for the TCGA data into four groups—Neural, Proneural, Mesenchymal and Classical—was obtained from <https://genome-cancer.ucsc.edu> (Verhaak et al., 2010). 466 patients had valid survival data. CDC20 expression in glioblastomas was normalized to the mean of the normal brain samples. The overall survival of patients with CDC20 expression level ≥ 2 times and < 2 times that of normal brain samples was compared using Kaplan Meier survival curves, and the log-rank test was performed. This analysis was performed on the data as a whole, as well as for each of the four molecular subtypes (IBM SPSS statistics (Version 21) software package). Maximally selected statistics on the derived linear predictor from a Cox proportional hazard model was used to identify an optimal OS cut-point for CDC20 expression while maintaining a minimum of 20% and a maximum of 80% of all patients in each group to avoid assigning too few patients to one group (Lausen et al., 2004). This analysis was performed on the data as a whole, as well as for individual molecular subtypes where indicated (IBM SPSS statistics (Version 21) software package). The TCGA Glioblastoma dataset has mutation data on 9658 genes in 291 patients. 15 IDH1 gene mutations (SNPs and missense) were identified in 15 independent patients. We restricted analysis to the 235 patients with available gene expression (Agilent G4502A gene expression microarray) and mutation data in the TCGA. Correlating subtype and IDH1 mutation data among these 235 patients, the Proneural subtype encompasses 49 patients in total with all of the IDH1 mutations (11 of 15) represented in the Proneural subtype as expected.

Supplemental References

Bhat, K.P., Balasubramaniyan, V., Vaillant, B., Ezhilarasan, R., Hummelink, K., Hollingsworth, F., Wani, K., Heathcock, L., James, J.D., Goodman, L.D., *et al.* (2013). Mesenchymal differentiation mediated by NF-kappaB promotes radiation resistance in glioblastoma. *Cancer cell* 24, 331-346.

Gross, S., and Piwnica-Worms, D. (2005). Real-time imaging of ligand-induced IKK activation in intact cells and in living mice. *Nature methods* 2, 607-614.

Kim, A.H., Yano, H., Cho, H., Meyer, D., Monks, B., Margolis, B., Birnbaum, M.J., and Chao, M.V. (2002). Akt1 regulates a JNK scaffold during excitotoxic apoptosis. *Neuron* 35, 697-709.

Lausen, B., Hothorn, T., Bretz, F., and Schumacher, M. (2004). Assessment of optimal selected prognostic factors. *Biometrical J* 46, 364-374.

SUPPLEMENTAL INFORMATION INVENTORY

Supplemental Data

Table S1. Clinical characteristics of glioblastoma tumors used to derive GSCs, Related to Figure 1.

Figure S1. Characteristics of human glioblastoma stem-like lines used in this study, Related to Figure 1.

Figure S2. CDC20-APC is required for human GSC invasiveness *in vitro*, Related to Figure 1.

Figure S3. The effect of molecular and pharmacological manipulations of CDC20-APC on cell cycle distribution, proliferation, cell death, and cell health, Related to Figure 1.

Figure S4. CDC20-APC controls SOX2 protein stability and SOX2-dependent transcription in GSCs, Related to Figure 3.

Figure S5. Visualization of GSC tumorigenicity *in vivo* by immunofluorescence, Related to Figure 4.

Figure S6. The impact of CDC20 expression on overall survival in the TCGA Glioblastoma dataset, Related to Figure 5.

Supplemental Experimental Procedures

Supplemental References